

MEMORANDUM

To: Dan Fabricant

From: Warren Brown

Date: 23 May 2002

Subject: Binospec Thermal Analysis II: Description of the Thermal Model

1. INTRODUCTION

This the second of a series of memos concluding the Binospec thermal analysis. This memo describes the details of the model and the calculations we did. The memo is arranged as follows:

Section 2: A mathematical review of the equations used in the heat transfer models. Examples illustrate the discrete node calculations and the view factor estimates.

Section 3: The Binospec finite difference models, and how I constructed them. I briefly describe the results of the detailed collimator and filter changer models.

Appendix A: Presents the organization and syntax of a Thermal Analysis Kit III input file.

2. MATHEMATICAL BACKGROUND

2.1. Heat Transfer Equations

As a brief review, heat transfer is energy in transit due to a temperature difference. There are three modes of heat transfer: conduction, convection, and radiation. The heat transfer rates q for these three modes are

$$Q_{conduction} = kA_x(T_1 - T_2)/L \tag{1}$$

$$Q_{convection} = hA(T_{air} - T_{surface}) \tag{2}$$

$$Q_{radiation} = \epsilon\sigma A(T_{env}^4 - T_{surface}^4), \tag{3}$$

TABLE 1
Symbols

Symbol	Description	Units
T	temperature	K
m	mass	kg
L	length	m
A	surface area	m ²
A_x	cross-sectional area	m ²
C	specific heat (at constant pressure)	J kg ⁻¹ K ⁻¹
k	conductivity	W m ⁻¹ K ⁻¹
h	convection coefficient	W m ⁻² K ⁻¹
σ	Stefan-Boltzmann constant	W m ⁻² K ⁻⁴
ϵ	emissivity	
F_{ij}	view factor	

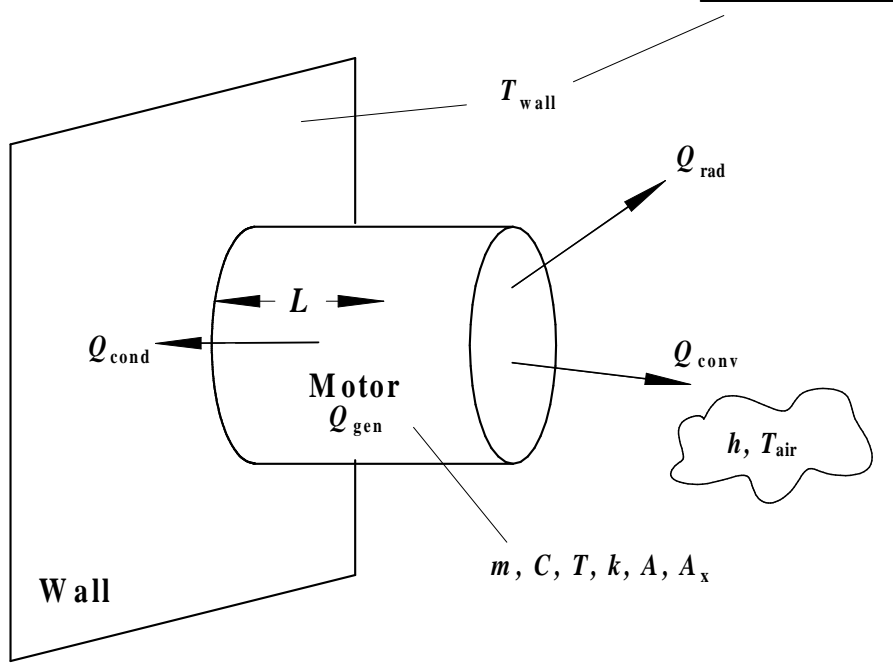


Fig. 1.— Energy balance example: conduction, convection, and radiation from a motor.

where the variables are defined in Table 1.

Conservation of energy governs the heat transfer process. The heat flow into a point Q_{in} plus the heat generated at that point Q_{gen} minus the heat flow out Q_{out} equals the net energy stored or lost Q_{stor} per unit time:

$$Q_{in} + Q_{gen} - Q_{out} = Q_{stor}. \quad (4)$$

The energy stored is related to an object's temperature, $q = mC(T_{final} - T_{initial})$.

Heat transfer calculations for complicated systems, like the Binospec spectrograph, are simplified by assuming components are lump masses with spatially uniform temperatures. For example, Figure 1 shows a motor as a single lump with mass m , specific heat C , conductivity k , cross-sectional area A_x , surface area A , and temperature T . Heat is generated in the motor Q_{gen} , conducted to a wall, radiated to the wall, and convected to the air. The energy balance equation for the Figure 1 example is:

$$Q_{gen} - (Q_{cond} + Q_{conv} + Q_{rad}) = mC \frac{dT}{dt}, \quad (5)$$

or substituting Equations 1 - 3,

$$Q_{gen} - \left[\frac{kA_x}{L}(T - T_{wall}) + hA(T - T_{air}) + \epsilon\sigma A(T^4 - T_{wall}^4) \right] = mC \frac{dT}{dt}. \quad (6)$$

We would like to solve equation 6 for T in order to know the motor temperature at all future times. However, equation 6 is a nonlinear, first-order, nonhomogeneous ordinary differential equation that cannot be integrated to obtain an exact solution.

Discrete time steps are used to numerically solve heat transfer equations for a finite difference model. The approximation to the time derivation is expressed as

$$\frac{dT}{dt} \approx \frac{T(t + \Delta t) - T(t)}{\Delta t}. \quad (7)$$

Temperatures are solved at times incremented by Δt , so that $t = n\Delta t$. The nature of the solution will depend on the specific time at which temperatures are evaluated. In Equation 7 the temperatures are evaluated at the *previous* time; this “forward-difference” approximation is used to solve the models presented here.

2.2. Finite Difference Model Example

I present a hypothetical Binospec lens bezel (see Figure 2) as a one-dimensional example of a finite difference model. For simplicity, the effects of convection and radiation are ignored. The goal of this example is to calculate how quickly heat conducts around a lens bezel from a focus motor attached to the base of the bezel.

The following three equations solve the heat transfer over time for the model in Fig. 2:

$$\text{node 1, bottom :} \quad Q_{gen} + 2\frac{kA_x}{\Delta x}(T_2(t) - T_1(t)) = mC\frac{T_1(t+\Delta t)-T_1(t)}{\Delta t} \quad (8)$$

$$\text{node 2, sides :} \quad 2\frac{kA_x}{\Delta x}(T_1(t) - T_2(t)) + 2\frac{kA_x}{\Delta x}(T_3(t) - T_2(t)) = 2mC\frac{T_2(t+\Delta t)-T_2(t)}{\Delta t} \quad (9)$$

$$\text{node 3, top :} \quad 2\frac{kA_x}{\Delta x}(T_2(t) - T_3(t)) = mC\frac{T_3(t+\Delta t)-T_3(t)}{\Delta t} \quad (10)$$

The factor of 2 arises in this example because node 2 includes both sides of the bezel; node 2 has twice the mass and cross-sectional area of nodes 1 and 3.

The temperature of the bezel nodes can be solved for all future times by re-arranging the equations to solve for the $T(t + \Delta t)$ variables. The accuracy of the forward-difference solution may be improved by decreasing the values of Δt and the node length Δx . The power of the motor Q_{gen} and the physical characteristics of the bezels m , C , k , and A_x are defined by the user.

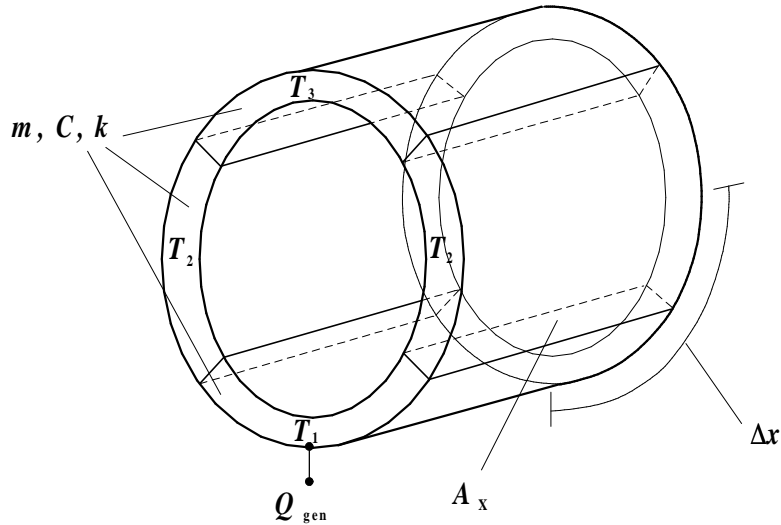


Fig. 2.— Finite difference model example: conduction around a lens bezel.

Evaluating Equations 8 - 10 for the Binospec collimator lens group 2 bezel, I find that if the focus motor is operated at 16 Watts for 1 minute, the node 1 temperature T_1 will initially rise 0.06° C and the three nodes will equilibrate after ~ 1.5 hours. This calculation assumes a $m = 16.8$ kg aluminum bezel with typical cross-section $A_x = 0.005$ m² and node length $\Delta x = 0.4$ m.

2.3. View Factors

Calculating radiation exchange requires the use of “view factors.” The view factor F_{ij} is the fraction of radiation leaving surface i that is intercepted by surface j .

Figure 3 shows two arbitrarily oriented surfaces A_i and A_j . Elemental areas dA_i and dA_j are connected by a line of length R , which forms the polar angles θ_i and θ_j , respectively, with the surface normals \hat{n}_i and \hat{n}_j . The view factor F_{ij} that connects A_i and A_j is given by

$$F_{ij} = \frac{1}{A_i} \int_{A_i} \int_{A_j} \frac{\cos \theta_i \cos \theta_j}{\pi R^2} dA_i dA_j \quad (11)$$

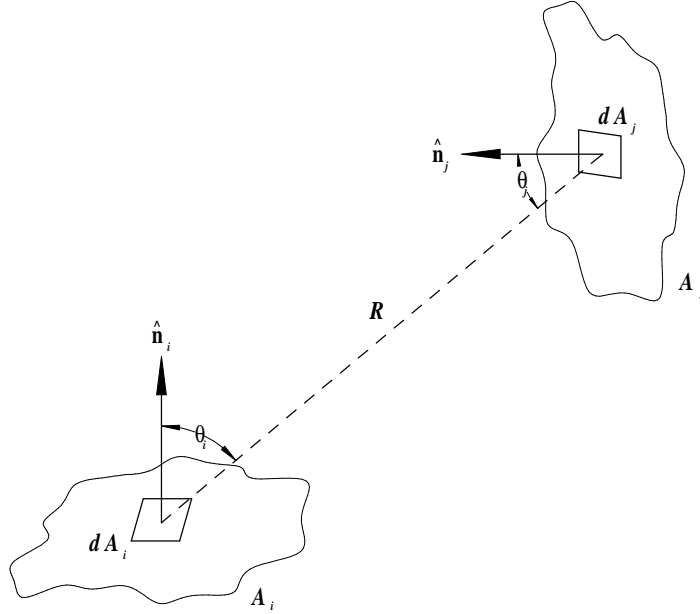


Fig. 3.— View factor.

The view factor has a value between 0 and 1. The sum of the view factors for a surface must equal one:

$$\sum_{j=1}^n F_{ij} = 1. \quad (12)$$

The view factor is also reciprocal, such that $A_i F_{ij} = A_j F_{ji}$.

In practice, simple geometries that can be integrated exactly are used to estimate view factors (see Figure 4). Useful relations include the view factor for perpendicular infinite plates with a common edge,

$$F_{ij} = \frac{1 + (j/i) - \sqrt{1 + (j/i)^2}}{2}, \quad (13)$$

and the view factor for coaxial parallel disks,

$$S = 1 + \frac{L^2 + j^2}{i^2} \quad (14)$$

$$F_{ij} = \frac{S - \sqrt{S^2 - 4(j/i)^2}}{2}. \quad (15)$$

These simple geometrical relations, combined with the properties of the view factor (Equation 12), allow quick estimates of view factors in the Binospec model.

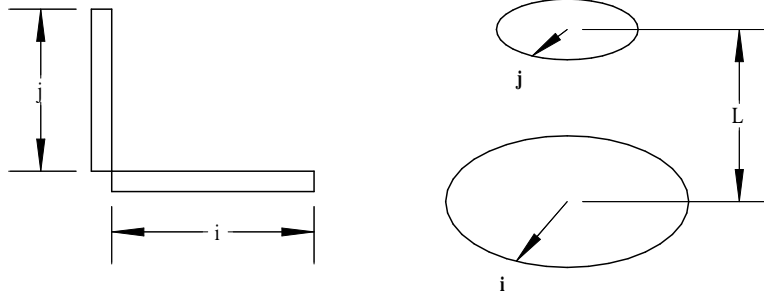


Fig. 4.— View factor geometries for 1) perpendicular infinite plates with a common edge (left) and 2) coaxial parallel disks (right).

2.4. View Factor Example

I present the view factors I used for collimator lens group 1 as an example of the view factor estimates made for the Binospec model. The i node is the top of collimator lens group 1 (node 164 in Figure 8). The j nodes are the Binospec elements (shown in Figure 5) hanging above collimator lens group 1.

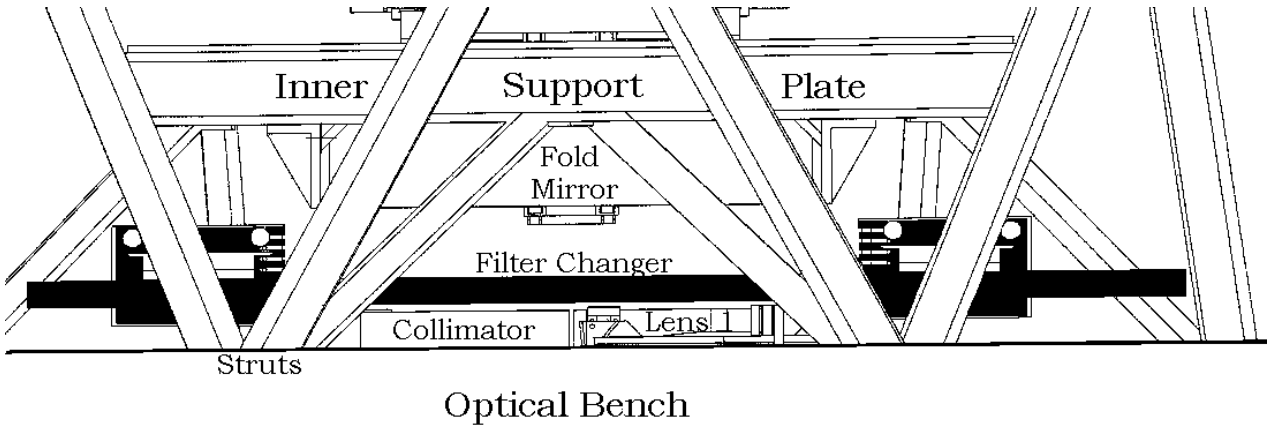


Fig. 5.— Binospec collimator lens 1 sits below the inner support plate, the fold mirror, and the filter changer (marked in black).

The lens node has a circular surface area $A_i = 0.035 \text{ m}^2$ ($i = 0.1 \text{ m}$) and conveniently matches the coaxial parallel disk geometry. For example, the fold mirror directly above collimator lens 1 has an effective radius $j \simeq 0.1 \text{ m}$. I estimate the fold mirror is $L \simeq 0.25 \text{ m}$ above collimator lens

1. Thus equations 14 - 15 give $S = 8.25$ and $F_{ij} = 0.12$. Because the central fold mirror sits off to one side of collimator lens 1, I estimate its view factor to be half that of the first fold mirror.

There is no simple relation to use for the filter changer geometry, so I turn to solid angles to estimate the view factors. The filter rails are 0.04 m wide and straddle collimator lens 1 approximately 0.1 m above the lens surface. Simple right triangles show that filter rails subtend the angles $37^\circ < \theta < 49^\circ$ (where θ is measured from the normal) from the center of the lens. The solid angle of this strip around a hemisphere is $\Omega = 2\pi \cos 37^\circ - 2\pi \cos 49^\circ = 0.15 \ 2\pi$. Thus the view factor is 0.15; I split this into $F_{ij} = 0.08$ for each rail.

The filter housing (that holds the filters) also sits adjacent to collimator lens 1. The geometry of this situation roughly matches the perpendicular plates with a common edge. I take the filter housing to be $j = 0.2$ m high and a distance $i = 0.2$ m from the center of collimator lens 1. Equation 13 yields a view factor of 0.29. I then subtract this view factor from the view factor of the $i = 0.1$ m next to the housing, 0.38. The remaining view factor is that due to the $i = 0.1$ m offset from the housing, $F_{ij} \simeq 0.09$.

The inner support plate is well matched to the coaxial parallel disk geometry. The $j = 0.6$ m plate sits $L = 0.35$ m above collimator lens 1 to give $S = 49$ and $F_{ij} = 0.74$. I subtract the 0.18 view factor of the fold mirrors and the 0.16 view factor of the filter rails to find that 0.40 remains for the inner support plate. The filter housing should not block a significant view of the inner support plate. The inner support plate is modeled with middle and edge nodes, and so I assign the middle node $F_{ij} = 0.25$ and the edge node $F_{ij} = 0.15$.

TABLE 2
View Factor example

j node	F_{ij}
Fold mirror	0.12
Center fold mirror	0.06
2 Filter changer rails	0.16
Filter changer housing	0.09
Inner support plate	0.40
	===
total:	0.83

I assign a total view factor of 0.83 to the collimator lens 1 node, 0.17 short of the full hemisphere. Table 2 summarizes the results. The total view factor should equal 1 if the view factors are perfectly accounted for. I do not assign radiative links to nodes with view factors less than 0.05 for computational efficiency. For example, radiative links between the collimator lens 1 and the individual graphite epoxy struts are ignored.

2.4.1. Accuracy of View Factors

The Binospec view factor estimates are based on hard numbers, but they are only estimates. Individual view factors may be off by 50% or 100%. However, the sum total view factor for a node

usually falls near 1. This implies the total radiative flux is correct, but noisy on a node-by-node basis.

The view factor inaccuracy is significant to the heat transfer calculations at the few percent level. Radiation accounts for approximately 25% of the heat flow on exposed nodes (for the temperature differences found in the Binospec model). In the above example, the collimator lens 1 node experiences on a peak 8.5 W of conduction, 3.5 W of convection, and 4.2 W of radiation. If a view factor of 0.2 is changed by 0.1 (50%), the heat flow on the node will change by 0.4 Watts, or 2.5% of the total heat flow. If all view factors for the collimator lens 1 node are systematically 2 times too large, the total heat flow will be 2.1 W, or $\sim 10\%$, too large.

3. THERMAL ANALYSIS KIT III MODELS

A finite difference model for a complicated system like the Binospec spectrograph requires hundreds of nodes, with each node connected conductively, convectively, and radiatively to dozens of other nodes. Writing out the heat transfer equations for such a complicated system is difficult. Thus I turn to David Boyd's Thermal Analysis Kit III (hereafter TAK) software, a professional heat transfer program. TAK calculates the heat transfer equations for a finite difference model specified in a text input file. The power of TAK is that it allows us to simply change and re-run a complicated model with different assumptions and boundary conditions.

Appendix A outlines the organization and syntax of a TAK input file.

I create three major TAK models: a low-resolution lump model of the entire Binospec system, and high-resolution models of the collimator and filter changer. Most of the heat transfer conclusions come from the general Binospec model, and so I focus on that model. The following sections describe the data the models are based on and how the models are constructed. The general Binospec model results are presented in the next memo.

3.1. Mechanical, Optical, and Environmental Data

The Binospec structural design was provided by Jack Barberis in September 2000. Detailed models exist for every component except for the dewar, grating changer, shutter, and coherent fiber assembly.

The Binospec optical data was provided by Dan Fabricant in September 2000. The Binospec collimator and camera are refractive designs made of 3 lens groups each. Material properties are tabulated in the Optics memo; glass information was obtained from Ohara, and the CaF_2 and NaCl data was obtained from Optovac.

The structural material properties used in the Binospec models are listed in Table 3. I assume Aluminum 6061 for the structural material throughout Binospec. The exceptions are the steel mounting flange, motors, and motor rails. The struts are graphite-epoxy, for which I use the isotropic conductivity $k = 36 \text{ W m}^{-1} \text{ K}^{-1}$ (the conductivity could be three times greater if non-isotropic). I assume an exterior insulation of 3 inch urethane foam with a 1 mm Aluminum skin.

Stepper motor properties are obtained from catalogs provided by Tom Gauron. I take the maximum output of a size 23 motor to be 16 Watts. Actual power output will be determined by individual usage. Dan Fabricant specifies motor actuation times and typical observing sequences at <http://cfa-www/mmti/mmti/wu/bino/elec.html>.

MMT dome temperatures were measured in May 2001 and provided by Steve West; the data is presented in the MMT Dome Temperature memo. “Typical” MMT dome temperature variations are $\pm 3^\circ\text{C}$ over 24 hours. “Extreme” temperature variations are $\pm 10^\circ\text{C}$ over 8 hours. The models use these temperatures as boundary conditions. Air properties are for air at 275 K at 2500 m elevation (<http://www.alma.nrao.edu/memos/html-memos/alma203/memo203.html>). The MMT operates in an average wind speed of 13 ± 7 mph (Milone, instrument database document #198).

TABLE 3
Material Properties

Material	ρ kg m ⁻³	k W m ⁻¹ K ⁻¹	C J kg ⁻¹ K ⁻¹
Aluminum 6061	2713	164	962
416 Stainless	7750	24.9	460
Graphite Epoxy	1800	36	840
Urethane foam	70	0.026	1045
Air (275 K, 2500m)	0.95	0.024	1007

Each node in the Binospec model is connected by conductive, convective, and radiative “conductors” G . Conductive values $G = kA_x/L$ are calculated by summing adjacent nodes’ conductivities in series:

$$\frac{1}{G_{1\leftrightarrow 2}} = \frac{1}{G_1} + \frac{1}{G_2} \quad (16)$$

$$\frac{1}{G_{1\leftrightarrow 2}} = \frac{L_1/2}{k_1 A_x} + \frac{L_2/2}{k_2 A_x} \quad (17)$$

Convective values $G = hA$ are calculated for the exposed surface area A of a node. Radiative values $G = \sigma\epsilon F_{ij}A$ use the surface area A and require an estimate of the view factor F_{ij} . The emissivity of black paint $\epsilon = 0.92$ is assumed for all structural surfaces.

3.2. Low-Resolution Binospec Model

The Binospec model boundary condition is a single **environment** node. The environment node has infinite mass. It is convectively and radiatively connected to the top, side, and bottom insulation nodes. I assume the telescope mounting surface is the same as the environment temperature, and conductively connect the environment node to the mounting flange node. The environment node temperature is specified by a temperature versus time (TVT) array. The temperatures used in the baseline model are MMT dome temperatures measured in May 2001 (Steve West).

The Binospec model **insulation** is broken into a bottom panel, three side panels, a top panel, and an entrance window. The baseline Binospec model assumes 3 inch thick urethane foam panels

with 1 mm aluminum skins. The entrance window has a pessimistic 28 inch diameter and 0.5 inch thickness. To properly allow for the large temperature gradient through the insulation, the foam panels and entrance window are modeled with three nodes each. One node represents the mass of the foam panel or window, and two massless nodes represent the interior and exterior surfaces. All other nodes in the Binospec model conduct, convect, or radiate to the massless surface nodes, which provide the correct temperatures for the insulation surfaces.

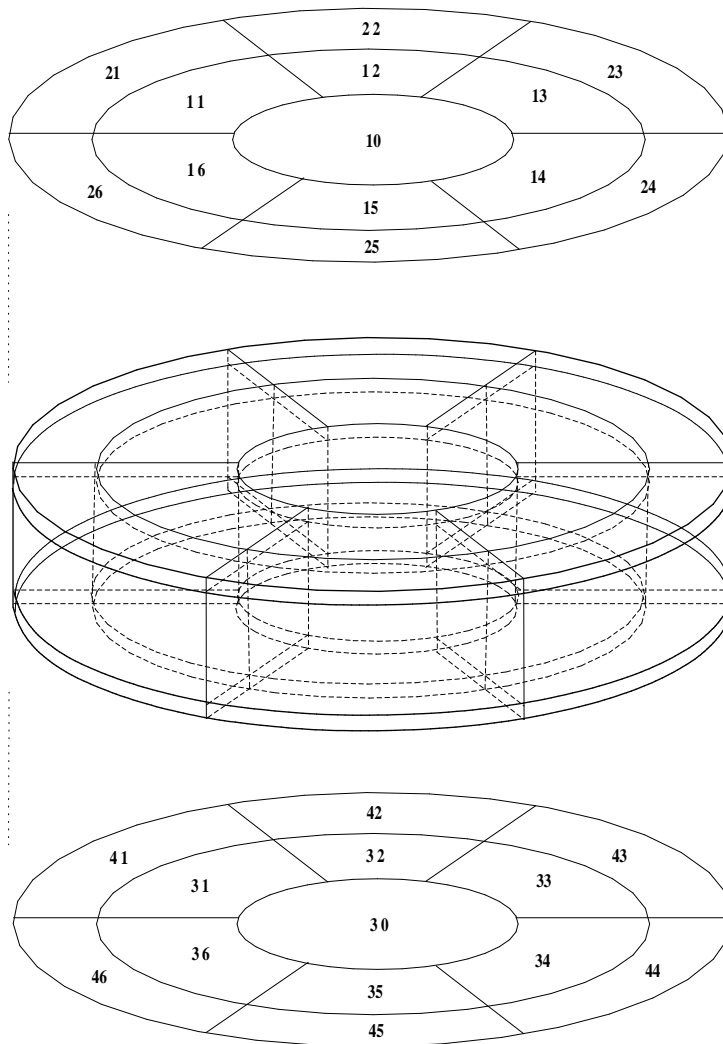


Fig. 6.— Optical bench node map (core nodes not listed for clarity), general Binospec model.

I assume the **optical bench** has 3/16 inch aluminum face sheets and a 6 inch aluminum honeycomb core. The face sheets and core are divided into 3 radial slices (with edges at $r_1 = 0.4$ m, $r_2 = 0.8$ m, and $r_3 = 1.07$ m) and into 6 angular slices, as shown in Figure 6. The core has conductivity $k = 5.4 \text{ W m}^{-1} \text{ K}^{-1}$ (Newport). I note that temperature gradients are more quickly transferred axially, through the optical bench, than radially or angularly along the face sheets — at least for the size of the nodes considered here. This is because the core density is down by the same factor as the conductivity and so the core thermal diffusivity is the same as the face plate.

The **air** is divided into 4 volumes by the Binospec spectrograph. Figure 7 shows the air nodes: 1) air below the optical bench, 2) air above the optical bench and below the inner support plate,

3) air above the inner support plate and below the entrance window, and 4) air above the entrance window and below the MMT mounting cone. In the baseline model, the convection coefficient inside the spectrograph is set to $h = 2$ for still air in an enclosed cavity. The air exterior to the spectrograph is simply the environment boundary node. I calculate an exterior convection coefficient $h = 18$ for a pessimistic 20 mph air flow around the cylindrical spectrograph (I use relations from the *Handbook of Heat Transfer Fundamentals*). The MMT operates in an average wind speed of 13 ± 7 mph (Milone).

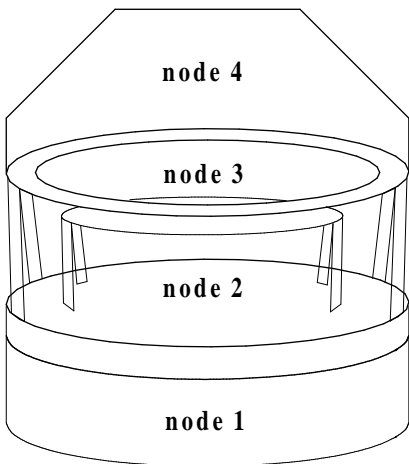


Fig. 7.— Air nodes, general Binospec model.

The **mounting flange** is modeled as a single node, and the twelve 0.96 m long **graphite epoxy struts** are paired up into six nodes. The graphite epoxy strut nodes connect the mounting flange to each node in the outer ring of the optical bench top face plate. I note that because the struts have relatively large surface areas and small cross-sectional areas, convection and radiation carry away a significant fraction of the heat flow along the struts.

The **inner support plate** (hereafter ISP) is modeled with a central node and two edge nodes. The support ring (going around the circumference of the ISP) is a single node, and is connected to the outer ring of the optical bench by six graphite epoxy strut nodes. I assume a thin aluminum shroud extends from the ISP up to the mounting flange. The **coherent fiber assembly** mounted on the ISP is simply modeled with two nodes for the rails and two nodes for the motors.

The **slit mask changer** and **filter changers** are based on Roger Eng’s design. The housing is lumped into a single node. The three rails on each assembly are assigned three separate nodes. The four motors per assembly are assigned separate nodes and attach to the rails. The baseline Binospec model assumes no thermal stand-offs or radiation shields for the motors.

The **fold mirror assembly** is modeled with 2 nodes for the structure. The fold mirrors are assigned individual nodes. I note that the conduction time constant of the fold mirrors is ~ 4 times longer than the convection time constant (because of the small conduction path provided by the mounting flexures). I do not consider air exchange through the fold mirror assembly because of the small cross-sectional area provided by the assembly and the slit masks.

The **collimator** and **camera** node maps are displayed in Figure 8. The lens groups are modeled with two axial slices (four in the case of collimator lens group 2) and two radial slices.

The conductivity and specific heat of a lens element is based on the optical prescription at that location. The RTV pads are calculated as part of the conductor between the lens groups and the bezels. Each bezel is modeled as a lump node. The collimator bezels connect to a few structural nodes and to the optical bench; the camera bezels connect to a single mount node. In the baseline model, the camera barrel node surrounds lens groups 1 and 2 and protects them from convection and radiation exchange with the spectrograph. I do account for radiation exchange between the surfaces of the lens groups.

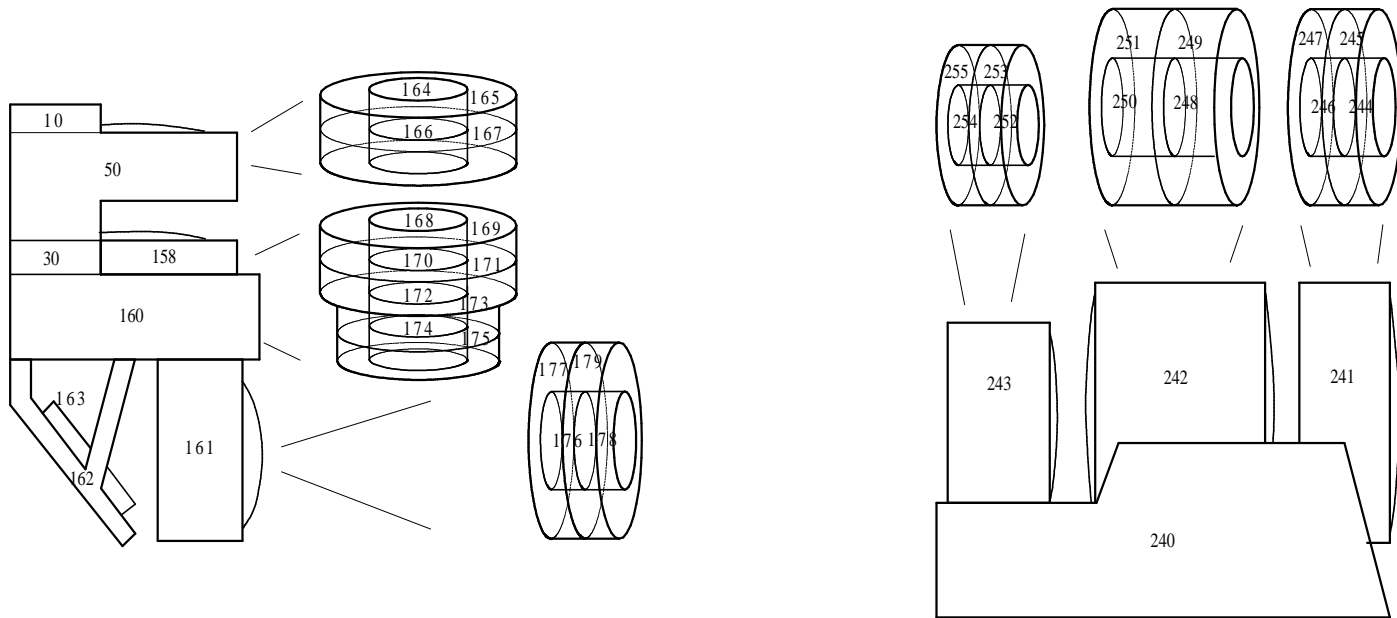


Fig. 8.— Node map of the collimator and camera, general Binospec model.

The **grating turrets** and **grating changers** are based on estimates made from Jack Barberis's drawings. The grating turret has nodes assigned to the grating, the grating mount, the grating turret structure, the fold mirror, and the two turret motors. The grating changer structure is similarly modeled. I note that the gratings interact with the spectrograph through convection and radiation exchange; the small delrin pads in the grating mounts provide a negligible conduction path.

There is no dewar design, so the **dewars** are represented as lump mass nodes. I assume 22 kg of aluminum with surface area 0.44 m^2 .

3.2.1. Model Calculations

The results of the general Binospec model are presented in the following memo.

3.3. Detailed Collimator Model

The detailed collimator model is designed to study temperature gradients in the optics. Each lens group is divided into 4 axial slices, 4 radial slices, and 8 angular slices for a total of 128 nodes

per lens group (see Figure 9). The bezels are divided into 4 axial slices and 8 angular slices, with the mass distributed appropriately among the nodes. The lens and bezel surfaces are conductively and radiatively connected to the rest of the spectrograph as the boundary condition. Separate boundary nodes are used above and below the optical bench, though the optical bench is otherwise ignored. The detailed collimator model was created independent of the general Binospec model.

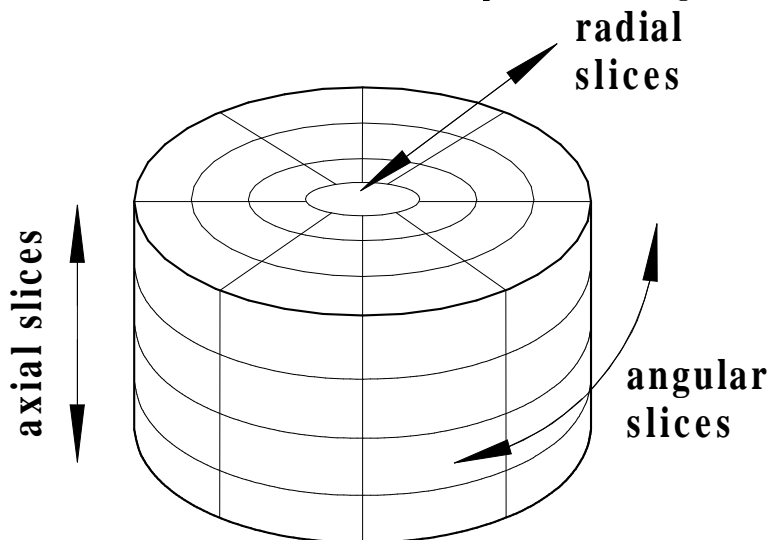


Fig. 9.— Example Binospec collimator lens group, used in the detailed collimator model. The radial and axial slices are necessary to measure radial and axial temperature gradients, respectively. The angular slices are necessary to measure asymmetric diametral gradients.

3.3.1. Model Calculations

The detailed collimator model was run with two different boundary conditions: a 10° C ramp over 10 hours, and air temperatures from the general Binospec model.

The 10° ramp reveals an asymmetric radial temperature gradient in the collimator lenses. The asymmetry arises because the lower halves of the collimator bezels have more mass than the upper halves, and because the lower halves are convectively and radiatively shielded by the collimator shroud. The top-to-bottom temperature gradient is 25-50% of the radial temperature gradient.

I find surprisingly good agreement with the low-resolution Binospec model results when I use the air temperature from the low-resolution Binospec model as the boundary condition for the detailed collimator model. The radial and axial temperature gradients in the lens groups are the same with two exceptions. The detailed model, which better models the collimator structure, finds 25% smaller radial gradients in lens group 2. The detailed model also finds 50% greater axial gradients in lens group 1, but the boundary conditions between the models differ most greatly for the top of lens group 1.

3.4. Detailed Filter Changer Model

The detailed filter changer model is based on the slit mask changer design of Roger Eng. The purpose of the filter changer model is to understand how hot the filter motors become. We are concerned about the filter motors because they may be operated every ~ 5 minutes in “imaging mode,” and have a direct line-of-sight to collimator lens 1.

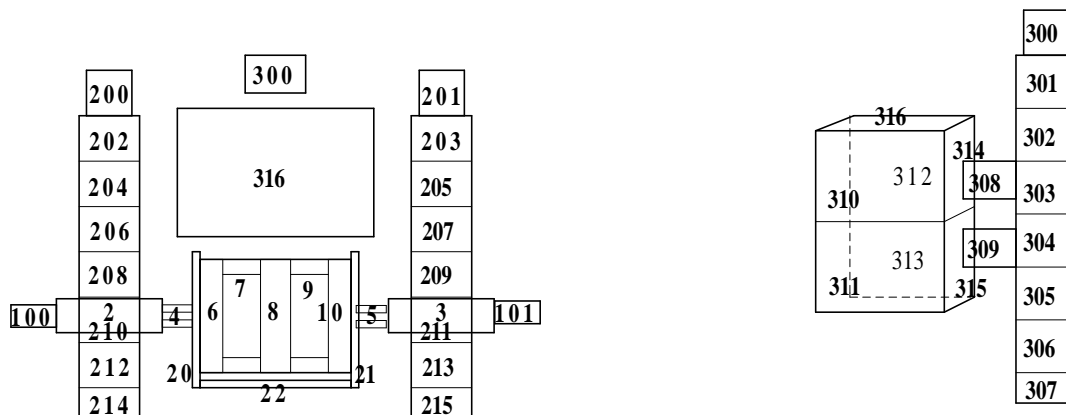


Fig. 10.— Node map of the detailed filter changer model.

The filter changer structure is broken into nodes as shown in Figure 10. The model contains 50 mass nodes with full convective and radiative coupling to the surrounding environment. Convection is dealt with by an air node that (convectively) connects to the mass nodes and to the spectrograph boundary node. I assume a constant boundary temperature in the following calculations.

3.4.1. Model Calculations

We assume a filter change every 5 minutes (“imaging mode”). In imaging mode, the detailed filter changer model confirms the 2° C temperature rise of the filter rail motor calculated by the general Binospec model. The other motors are found to rise $0.25 - 0.4^\circ$ C in imaging mode. The motors equilibrate with a time constant of 1 hour. A 1° C temperature gradient, with a time constant of ~ 1.5 hours, is induced in the filter rail. There is a negligible temperature gradient across the filter cartridge.

We also calculate the equilibrium motor temperatures if they are accidentally left on continuous full power for 24 hours. If left on, the small engage/dis-engage motors will rise 13° C with a time constant of 1 hour. These motors will induce a 0.6° C center-to-edge temperature gradient across the filter cartridge. The rail motor, if sunk directly to the rail, will rise 35° C with a time constant of 1 hour. The THK rail will be heated 20° C. If the rail motor is placed on stand-offs, the rail temperature only rises 3° C but the motor temperature rises a total of 46° C. The filter cassette motor acts very similarly to the rail motor. These numbers come from an iterative calculation in which the convection coefficient is re-calculated as the motor temperature rises (h reaches 6).

A. TAK III: ORGANIZATION AND SYNTAX

The TAK input files are divided into a series of data blocks. The values given in the following paragraphs are those used in the general Binospec model. I begin with some general statements.

The input file is not case sensitive, but the first letter of a word is important. Floating point variables must begin with A-H or O-Z; variables beginning with I-N are integers. Floating point numbers must use a decimal point at all times. Lines with C in the first column are comment lines. The dollar sign serves as a comment and identifier for that input line.

HEADER OPTIONS DATA. This section starts the TAK file. The options section specifies the solution algorithm (SOLRTN = FWDWRD), units (UID = SI), and printing options. A useful printing option is QDUMP = ON, which prints the heat flow network at the ending time. The option LODTMP = ON allows you to use the previous output file to provide the initial temperatures for the next program run.

HEADER CONTROL DATA. This section controls the calculation times and allows user defined constants. DTIMEI overrides the automatic time step, TIMEND = 36000.0 sets the ending time at 10 hours, OUTPUT = 1200.0 sets the output file to write every 20 minutes, and PLOT = 1200.0 sets the plot file to write every 20 minutes. User defined variables look like $PI = 3.14159$ or $AREA = PI * R * R$.

HEADER NODE DATA. This section creates the nodes. The nodes are specified by: NODE #, T_{init} , mC . Node numbers that are negative have infinite mass (i.e. the telescope dome environment); nodes with positive node numbers but negative thermal capacitances mC have zero mass (i.e. the surface of the insulation). Nodes with the same initial temperature and thermal capacitance can be specified by: NODE #, NUM NODES, INC, T_{init} , mC . A node's temperature can be specified in time with: TVT NODE #, ARRAY #.

HEADER CONDUCTOR DATA. This section connects all the nodes. The conductors are specified by: COND #, NODE 1, NODE 2, VALUE. The value of the conductor is kA_x/L for conduction, hA for convection, and $\sigma\epsilon F_{ij}A$ for radiation. Radiation conductors have negative conductor numbers; σ should be removed if SIGMA = 5.67E-08 is set in the Header Control Data section. Multiple conductors can be specified by: COND #, NUM COND, INC, NODE 1, INC, NODE 2, INC, VALUE.

HEADER ARRAY DATA. This sections contains the data for the temperature arrays. An array is specified by: ARRAY #, TIME 0, TEMP 0, TIME 1, TEMP 1, ... , TIME N, TEMP N, END. Do not use a comma at the end of a line in a multi-line array.

HEADER SOURCE DATA. This section allows heat generation in nodes. A constant heat source is specified by: NODE #, Q. The heat Q is in Watts (in SI). A periodic heat source (i.e. the stepper motors) is specified by: STF NODE #, TIME ON, TIME OFF, PERIOD, Q. The on/off times and cycling period are in seconds (in SI).